

Title: **Alpha 1-antitrypsin mitigates the inhibition of airway epithelial cell repair
by neutrophil elastase**

Character count with spaces: 100/100

Running: **A1AT mitigates inhibition of pAEC repair by NE**

Character count with space: 46/50

Authors: Luke W Garratt^{1,2}, Erika N Sutanto^{2,3}, Kak-Ming Ling², Kevin Looi¹, Thomas
Iosifidis^{1,4}, Kelly M Martinovich², Nicole C Shaw², Alysia G Buckley^{2,5},
Elizabeth Kicic-Starcevich^{2,3}, Francis J Lannigan^{1,6}, Darryl A Knight^{7,8,9},
Stephen M Stick^{1,2,3,4} & Anthony Kicic^{1,2,3,4*} on behalf of AREST CF^{2,3,10,11,#}

¹*School of Paediatrics and Child Health, University of Western Australia, Nedlands, 6009,
Perth, Western Australia, Australia*

²*Telethon Kids Institute, University of Western Australia, Nedlands, 6009, Perth, Western
Australia, Australia*

³*Department of Respiratory Medicine, Princess Margaret Hospital for Children, Perth, 6001,
Perth, Western Australia, Australia*

⁴*Centre for Cell Therapy and Regenerative Medicine, University of Western Australia,
Nedlands, 6009, Perth, Western Australia, Australia*

⁵*Centre for Microscopy, Characterisation and Analysis, University of Western Australia,
Nedlands, 6009, Perth, Western Australia, Australia*

⁶*School of Medicine, Notre Dame University, Fremantle, 6160, Perth, Western Australia,
Australia*

⁷*School of Biomedical Sciences and Pharmacy, University of Newcastle, Callaghan, 2308, New South Wales, Australia*

⁸*Priority Research Centre for Asthma and Respiratory Disease, Hunter Medical Research Institute, Newcastle, 2305, New South Wales, Australia*

⁹*Department of Anesthesiology, Pharmacology and Therapeutics, University of British Columbia, Vancouver, V6T 1Z4, British Columbia, Canada*

¹⁰*Department of Respiratory Medicine, Royal Children's Hospital, Parkville, 3052, Melbourne, Victoria, Australia*

¹¹*Murdoch Childrens Research Institute, Parkville, 3052, Melbourne, Victoria, Australia*

Author's Contributions: Conception and design of the study – L.W.G., E.N.S., S.M.S., A.K.; sample acquisition and processing – L.W.G., K.M.L., K.L., T.I., K.M.M., N.C.S., E.K.S., F.J.L.; acquisition, analysis and interpretation of data – L.W.G., E.N.S., D.A.K., S.M.S., A.K.; drafting the article or revising it critically for important intellectual content – L.W.G., E.N.S., K.M.L., K.L., T.I., K.M.M., N.C.S., A.G.B., E.K.S., F.J.L., D.A.K., S.M.S., A.K.

**Corresponding author: Associate Professor Anthony Kicic, Telethon Kids Institute, Subiaco, Perth, 6008, Western Australia, Australia. Ph: (618) 9340 8140, Fax: (618) 9340 7429. email: Anthony.Kicic@telethonkids.org.au*

#The full membership of the Australian Respiratory Early Surveillance Team for Cystic Fibrosis (AREST CF) is available at <http://www.arestcf.org>.¹

Word count: 4,483/5,000

Funding for the AREST CF program was obtained from the Cystic Fibrosis Foundation Therapeutics (SLY04A0, STICK09A0), the National Health and Medical Research Council of Australia (NHMRC; Centre of Research Excellence #1000896) and project grant funding from the NHMRC and Cystic Fibrosis Australia (NHMRC 1043768). Stephen M Stick is a NHMRC Practitioner Fellow. Luke W Garratt is funded by a PhD scholarship from the NHMRC and supplementary scholarships from the University of Western Australia and Cystic Fibrosis Western Australia.

ABSTRACT:**Abstract word count:** 248/250

Neutrophil elastase (NE) activity is associated with many destructive lung diseases and is a predictor for structural lung damage in early cystic fibrosis (CF), which suggests normal maintenance of airway epithelium is prevented by uninhibited NE. However, limited data exists on how the NE activity in airways of very young children with CF affects function of the epithelia. The aim of this study was to determine if NE activity could inhibit epithelial homeostasis and repair and whether any functional effect was reversible by antiprotease alpha 1-antitrypsin (α 1AT) treatment. Viability, inflammation, apoptosis and proliferation were all assessed in healthy non-CF and CF pediatric primary airway epithelial cells (pAEC_{non-CF} and pAEC_{CF} respectively) during exposure to physiologically relevant NE. In addition, the effect of NE activity on pAEC_{CF} wound repair was also assessed. We report that viability after 48 hours was significantly decreased by 100 nM NE in both pAEC_{non-CF} and pAEC_{CF}, due to rapid cellular detachment that was also accompanied by inflammatory cytokine release. Furthermore, both phenotypes initiated an apoptotic response to 100 nM NE while \geq 50 nM NE activity significantly inhibited proliferative capacity of cultures. Similar concentrations of NE also significantly inhibited wound repair of pAEC_{CF} but this was reversed by the addition of α 1AT. Collectively, our results demonstrate free NE activity is deleterious for epithelial homeostasis and supports the hypothesis that proteases in the airway contribute directly to CF structural lung disease. It also highlights the need to investigate antiprotease therapies in early CF disease in more detail.

Keywords: neutrophil elastase, cystic fibrosis, primary cell culture, wound repair, alpha-1 antitrypsin

List of abbreviations:

α 1AT	alpha-1 antitrypsin
AREST CF	Australian respiratory early surveillance team for cystic fibrosis
BALf	bronchoalveolar lavage fluid
CF	cystic fibrosis
CFTR	cystic fibrosis transmembrane conductance regulator
CT	computed tomography
ECM	extracellular matrix
LDH	lactate dehydrogenase
MMP	matrix metalloproteinase
NE	neutrophil elastase
pAEC	primary airway epithelial cell
ssDNA	single-stranded DNA
UG	Ultroser G

INTRODUCTION:

Cystic fibrosis (CF) is a life-threatening, multi-organ genetic disease that culminates in pulmonary failure. Abnormal lung function and structural lung disease are evident as early as three months (1). Proteases including neutrophil elastase (NE) and matrix metalloproteinases (MMP) are powerful modifiers of tissues and extracellular matrix and have been implicated in contributing to structural CF airway disease (2). Present early in CF (3, 4), the argument that NE drives lung disease has been further strengthened by observations from the Australian Respiratory Early Surveillance Team for CF (AREST CF) program that uninhibited NE activity in bronchoalveolar lavage fluid (BALf) from infants is a strong predictor for development of bronchiectasis (5). The progressive nature of CF structural lung disease (6) suggests an inability of airway tissue to effectively repair in response to chronic injury. Thus, identifying and treating the mechanisms of poor airway repair in CF could potentially reduce long-term lung morbidity and mortality.

Although NE has been associated with lung morbidity (7) and the use of BALf has significantly improved understanding of pediatric CF lung disease (8), there is paucity of data as to whether levels of NE seen in very early CF can sufficiently damage the epithelium, alter tissue homeostasis and prevent effective repair. Investigations into the contribution of NE to pediatric CF lung disease have been limited due to difficulties in studying airways of infants and young children, as well as the multi-factorial nature of established inflammation. Primary airway epithelial cell (pAEC) cultures provide an insightful *in vitro* model of CF epithelial physiology and pediatric pAEC from children with mild disease can provide an ideal culture model of naïve CF epithelium, since adolescent and adult CF lungs typically altered feature morphology reflecting the established, severe neutrophilic disease (9). However, the majority of studies investigating mechanisms of NE damage have employed adult-derived, non-CF

epithelial cell lines ([10-19](#)) or pAEC derived from adults without CF ([16](#), [18](#), [20-22](#)). To our knowledge, no study has modelled pediatric pAEC exposure to levels of free NE activity that reflect early CF disease.

A routine program of pAEC collection by lower airway brushing of young children with and without airway disease, including asthma and CF ([23](#), [24](#)), has successfully allowed investigation of wound repair in pediatric inflammatory airway diseases ([25-27](#)). The aim of the study was to use this primary cell model system to measure repair responses of pAEC during concentrations of NE typically found in BALf of young children with CF. The two hypotheses that were specifically tested were: (i) the concentration of chronic NE exposure seen in early life CF will have a detrimental effect on pAEC function, including viability, apoptosis, inflammatory cytokine production and proliferation; (ii) that NE will inhibit wound repair of CF pAEC in a manner dependent on protease activity and reversible by exogenous inhibition of NE activity by alpha-1 antitrypsin (α 1AT).

Some of the results of these studies have been previously reported in the form of abstracts ([28](#), [29](#)).

MATERIALS AND METHODS: 397/500

Please refer to the online supplement for full details of methods.

Subjects and Cell Isolation

This study was approved by Human Ethics Committees at the Princess Margaret Hospital for Children, Perth, Australia, the Royal Children's Hospital, Melbourne, Australia and the St John of God Hospital, Perth, Australia. As described previously ([23](#), [25](#), [27](#)), lower airway pAECs were collected by bronchial brushing from 9 healthy, non-diseased pediatric controls, who were undergoing non-respiratory related elective surgery and 16 young children with CF who were participating in their annual clinical assessment including BALf. Subject demographics are provided (Supplementary Table 1). Primary cultures were established and classified as healthy, non-cystic fibrosis (pAEC_{non-CF}), or cystic fibrosis (pAEC_{CF}). Immortalized human bronchial epithelial cell lines NuLi-1 and CuFi-1 from adults (ATCC, Manassas, VA, USA) were used to optimise all cell experiments performed. Cystic fibrosis transmembrane conductance regulator (CFTR) genotype was determined as part of newborn screening. Bronchiectasis was detected by computed tomography (CT) and scored as previously described ([1](#), [5](#)). Lower respiratory pathogens were detected by clinical microbiological culture of BALf at the Princess Margaret Hospital for Children, Perth, Australia. NE activity was measured in BALf via a modified enzymatic assay ([30](#)).

Epithelial Homeostasis

The effect of NE on the epithelium was modelled via exposure of pAEC monolayers to purified human sputum NE (Elastin Products Company, Owensville, MO, USA). Cell

viability, proliferation, apoptosis and wound repair were assessed using both in-house and commercial assays, as outlined in the online supplement.

Epithelial Wounding

To assess wound repair kinetics, linear scratch wounds were created using a commercial monolayer wounding kit ([31](#)) and wound closure in the presence of NE was calculated through image analysis by the accompanying live-cell imaging system (Essen Bioscience, Ann Arbor, MI, USA), as outlined in the online supplement. For some experiments, NE activity was inhibited by 1 μ M α 1AT (Athens Research & Technology, Athens, GA, USA) to model aerosol antiprotease therapy.

Statistical analysis

Data were tested for population normality as well as homogeneity of variance by histogram plots and D'Agostino-Pearson omnibus test. Normally distributed data are reported as mean with \pm standard deviation and non-normally distributed data reported as median with interquartile range. Tests with appropriate parametric or non-parametric statistical analyses were conducted using GraphPad Prism 5, with *p* values less than 0.05 considered significant. Unless noted, experiments were performed in replicate using at least four patients of each cohort per experiment.

RESULTS:

Establishment of neutrophil elastase dose range:

A total of 1,338 BALf samples from 318 children with CF had routinely been assessed for free NE activity (Supplementary Table 2). Stratification by age revealed that prevalence of NE activity also increased with age, rising from 30.17% in the first year of life to 40.43% by age six. Over the same time span, mean free NE activity also increased from 20.24 nM in infancy to 116.41 nM by age six. When samples with detectable NE activity were solely assessed, a mean concentration of 62.61 nM free NE was measured in the first year and this value rose to 284.01 nM at age six. Thus a concentration range of 0-100 nM NE activity was deemed relevant for all subsequent *in vitro* experiments performed.

Attachment and viability:

Exposure of pAEC monolayers to NE over 48 hours resulted in significant loss of confluence and increased cell detachment of viable cells (Figure 1). Compared to control media, incubation of both pAEC_{non-CF} and pAEC_{CF} with 100 nM NE resulted in a more spherical cellular morphology that was paralleled by significant detachment off the culture surface (Figure S1). Even as early as 12 hours of exposure to 100 nM NE, loss of confluence was significant for both pAEC_{non-CF} ($p < 0.01$; Figure 1A) and pAEC_{CF} ($p < 0.05$; Figure 1B) and this was maintained for the duration of the experiment. No significant morphological changes were observed for either phenotype at lower concentrations of NE. The number of viable attached cells in the monolayer was subsequently assessed by MTS colorimetric assay. When compared to control media, exposure to 100 nM NE resulted in a significant reduction in cell viability (Figure 1C) of both pAEC_{non-CF} (21.62% of control, $p < 0.001$) and pAEC_{CF} (40.02%

of control, $p < 0.05$). However, there was no significant difference in the reduced viability between pAEC_{non-CF} and pAEC_{CF} ($p = 0.4347$). Due to the significant loss of attachment, cellular viability was further investigated by measuring lactate dehydrogenase (LDH), a marker of cytotoxicity. There was a significant increase in supernatant LDH levels following 48 hour exposure to 100 nM NE for pAEC_{non-CF} ($p < 0.01$; Figure 1D), but not for pAEC_{CF}. Furthermore, there was no significant difference in LDH levels between pAEC_{non-CF} and pAEC_{CF} supernatant. When primary cells were compared to their equivalent cell lines, confluence measurements did not change over 48 hours for either NuLi-1 (Figure S2A) or CuFi-1 (Figure S2B) and suggested a reduced susceptibility to NE. There was also no significant change in viability (Figure S2C) or LDH production (Figure S2D) for either NuLi-1 or CuFi-1 when exposed to any concentration of NE.

Apoptosis:

Since no significant increase in cell cytotoxicity was observed to accompany the change in morphology and cell detachment, pAEC were then assessed for an apoptotic response to NE. Apoptosis was induced (2.48 ± 0.86 fold change over untreated) as early as three hours in pAEC_{non-CF} when exposed to 100 nM NE (Figure 2A; $p < 0.01$) and reached a peak of 3.50 ± 1.79 fold change at 12 hours ($p < 0.05$). In comparison, apoptosis in pAEC_{CF} was induced to a lesser extent by 100 nM NE with a significant apoptotic response (2.01 ± 0.65 fold change over untreated) only seen at 6 hours incubation (Figure 2B; $p < 0.05$). Although data suggested a lower apoptotic response in pAEC_{CF}, it was not significantly different to pAEC_{non-CF} at any time point assessed. Compared to their primary cell counterparts, no significant induction of apoptosis was observed for either NuLi-1 or CuFi-1 when exposed to similar concentrations of NE (data not shown).

Inflammatory cytokine production:

To investigate the relationship between NE exposure and inflammation, sentinel pro-inflammatory cytokines, IL-6 and IL-8 were measured in supernatants collected following the viability and apoptosis experiments (Figure 2C & 2D). There was no significant increase in IL-6 production by pAEC_{non-CF} after exposure to any of the NE concentrations assessed (Figure 2C). However, pAEC_{non-CF} produced significantly more IL-8 in response to 100 nM NE (145.26 ± 85.26 ng/mL/viable cells, $p < 0.01$) compared to controls (55.16 ± 21.45 ng/mL/viable cells). In contrast, exposure of pAEC_{CF} to 100 nM NE significantly increased IL-6 (32.08 ± 18.19 vs 13.47 ± 8.20 ng/mL/viable cells, $p < 0.05$) and IL-8 production (183.30 ± 127.60 vs 67.47 ± 39.84 ng/mL/viable cells, $p < 0.05$) compared to controls. When IL-6 and IL-8 levels were compared between disease phenotype, no differences were observed. When primary cell cultures were compared to cell lines, no significant induction of either IL-6 or IL-8 was observed for NuLi-1 or CuFi-1 when exposed to similar concentrations of NE (data not shown).

Proliferation:

Having established that exposure to free NE decreased pAEC viability, the effect on proliferation was assessed by counting cell number after 120 hour incubation and measuring viable cell number by MTS assay. When exposed to 10 nM NE, both pAEC_{non-CF} and pAEC_{CF} exhibited normal pAEC morphology and confluence increased over 120 hours (Figures 3A & 3B, S3 & S4). Interestingly, 50 nM NE inhibited this increase in confluence of both pAEC_{non-CF} (0.92 ± 0.21 vs 2.12 ± 0.55 fold, $p < 0.05$; Figure 3A & S3) and pAEC_{CF} (1.10

± 0.27 vs 2.23 ± 0.44 , $p < 0.01$; Figure 3B & S4), despite no apparent changes in cell morphology or attachment. Furthermore, no cell growth was observed when cells were exposed to 100 nM NE (Figure 3C) and final cell number of both phenotypes was significantly reduced in comparison to control media (pAEC_{non-CF} 13.51 ± 2.44 vs $5.23 \pm 2.09 \times 10^5$ cells, $p < 0.05$; pAEC_{CF} 10.86 ± 2.47 vs $5.19 \pm 0.91 \times 10^5$ cells, $p < 0.05$). Viable cell number after 120 hours also agreed with the confluence and cell number measurements (Figure 3D). Incubation with either 50 or 100 nM NE, significantly reduced the number of viable pAEC_{non-CF} and pAEC_{CF} when compared to controls (50 nM $p < 0.01$; 100 nM $p < 0.001$). Overall, a dose-dependent inhibition of proliferation was observed for both pAEC_{non-CF} and pAEC_{CF}, whereby 50 nM NE inhibited proliferation, while 100 nM abolished both attachment and proliferation of pAEC. In cell lines, both NuLi-1 and CuFi-1 were able to maintain attachment even in response to 100 nM NE with no significant change in morphology (data not shown). In addition, no significant effect on proliferation was seen after exposure to any concentration of NE assessed (Figure S5A-S5C).

Wound Repair:

Since NE is not typically detectable in healthy lungs where injury and inflammation is minimal, wound repair experiments were performed only in pAEC_{CF}. Exposure of wounded pAEC_{CF} monolayers to NE over 72 hours resulted in significantly delayed or inhibited repair (Figure 4). In non-NE exposed controls, rapid migration of cells into the denuded area was seen, with $50.30\% \pm 18.04$ of the wounded area confluent by 12 hours. Complete closure occurred at approximately 48 hours post wounding. There was no apparent effect on repair kinetics following exposure to 10 nM NE. In contrast, exposure to 100 nM NE significantly reduced closure to $15.45\% \pm 6.62$ ($p < 0.01$) by 12 hours. Cells exhibited rounded-up spherical

morphology and loss of attachment was observed in the non-wounded areas. Loss of adhesion was seen to persist for the period of incubation with NE. Passive migration of detached pAEC into the wound area through Brownian motion was limited by employing an automated, incubated microscope that eliminated plate movement. Resulting data for 100 nM NE exposure demonstrated that wound closure was incomplete at 21.48% \pm 6.90 by 72 hours (Figure 4; $p < 0.05$). A dose-dependent effect on repair was apparent, since 50 nM NE activity did not reduce attachment but did result in a slower repair rate, with wound closure at 30 hours significantly less (65.88% \pm 15.59) than controls (85.14% \pm 10.81; $p < 0.05$). However, repair was not completely inhibited but rather delayed, as wounds achieved full closure by 72 hours (Figure 4). In contrast to the primary cell data, 100 nM NE only delayed wound repair of CuFi-1 cells (Figure S7) up to 42 hours post-wounding ($p < 0.05$) and complete repair was still achieved by 72 hours.

NE Inhibition and Wound Repair

Having established that certain concentrations of free NE inhibited wound closure of pAEC_{CF}, the addition of NE inactivators such as α 1AT was investigated. Due to the significant reduction in wound closure, as well as morphological changes, after 12 hours exposure to 100 nM NE (Figure 4), this time point was selected for the addition of 1 μ M α 1AT. Cell morphology and wound closure was not affected by 1 μ M α 1AT (Figure 5A), either at 30 hours (91.42% \pm 7.63 closure in 1 μ M α 1AT vs 85.14% \pm 10.81 in control media, $p = 0.3194$) or 72 hours (99.57 \pm 0.97 closure in 1 μ M α 1AT vs 100.00 \pm 0.71 in control media, $p = 0.4428$). When 1 μ M α 1AT was added at 12 hours to pAEC_{CF} exposed to 100 nM NE, morphological and cell count assessment indicated cell attachment was restored (Figure S6). Closure at 30 hours post wounding by pAEC_{CF} initially exposed to 100 nM NE and then

treated with 1 μ M α 1AT was significantly increased over 100 nM NE alone (38.48% \pm 10.03 closure in 100 nM NE and 1 μ M α 1AT vs 20.22% \pm 6.55 in 100 nM NE and no α 1AT, $p < 0.05$; Figure 5B). Repair continued over the duration of the experiment, with a mean wound closure at 72 hours more than four-fold higher than cells not treated with α 1AT (79.94% \pm 17.50 closure in 100 nM NE and 1 μ M α 1AT vs 21.48% \pm 6.90 in 100 nM NE and no α 1AT, $p < 0.001$). Despite this improvement, wound closure at 72 hours for cells exposed to 100 nM NE and 1 μ M α 1AT still remained significantly lower than for pAEC_{CF} in control media alone (79.94% \pm 17.50 closure in 100 nM NE and 1 μ M α 1AT vs 100.00% \pm 0.71 in control media, $p < 0.05$; Figure 5B). For pAEC_{CF} exposed to 50 nM NE, addition of 1 μ M α 1AT also significantly increased repair at 24 hours compared to 50 nM NE alone (71.91% \pm 7.70 closure in 50 nM NE and 1 μ M α 1AT vs 56.51% \pm 13.59 in 50 nM NE and no α 1AT, $p < 0.05$). At 30 hours post wounding, closure was still significantly higher than for untreated cells (83.94% \pm 10.63 closure in 50 nM NE and 1 μ M α 1AT vs 65.88% \pm 15.59 in 50 nM NE and no α 1AT, $p < 0.05$) and was not significantly lower than pAEC_{CF} in control media ($p = 0.6716$). Interestingly CuFi-1 cells failed to recapitulate the improved repair seen in primary cells after addition of 1 μ M α 1AT (Figure S7).

Assessment of viable cell number at the end of wound closure experiments demonstrated that 100 nM NE led to a reduced viable cell number (14.19% \pm 7.07, $p < 0.001$; Figure 6) compared to controls. After 72 hours incubation with α 1AT, pAEC_{CF} viable cell number was significantly increased when 1 μ M α 1AT was added at 12 hours (71.95% \pm 11.55, $p < 0.001$), suggesting cellular detachment. However, viable cell number following α 1AT treatment was still lower than pAEC_{CF} in control media alone ($p < 0.05$). There was no significant effect of α 1AT on viable cell number for any of the lower NE concentrations assessed.

DISCUSSION:

This study investigated the response of pAEC cultures derived from pediatric patients with CF to concentrations of NE activity found in the airways and provides the first direct evidence that free NE adversely affects epithelial repair following injury. We comprehensively assessed the effect of NE purified from human CF sputum on the processes essential for epithelial homeostasis, namely; attachment, viability, apoptosis, proliferation and wound repair. Our data indicated that free NE activity was significantly deleterious for all of these processes, at relatively low concentrations found in BALf from infants with CF. Specifically, we found NE reduced both attachment and proliferation of pAEC, induced apoptosis and also inhibited the ability of cell culture monolayers to repair a scratch wound. Of significance was that subsequent addition of α 1AT mitigated the inhibitory effect of NE on reparative capacity, suggesting a potential therapeutic role for antiproteases in preventing tissue damage. This is the first age-relevant data to demonstrate that free NE activity impairs both homeostasis and wound repair of pAEC monolayers, further reinforcing a role for NE in the development of structural CF lung disease during infancy.

In order to identify concentrations of NE activity relevant to the early CF airway, we analysed a large, longitudinal cohort of more than 1,300 BALf samples. Overall, ~33% of BALf samples had free NE detected and within the first year of life, prevalence was ~30% with a mean NE activity of 62.61 nM. Although slightly lower than the 38-56% prevalence reported elsewhere ([3](#), [4](#), [32](#)), this is the first, unselected total cohort study reported. Both prevalence and mean level of NE activity was found to increase with age. Large variations in NE activity were also observed, with micromolar concentrations of activity in some samples

that approached adolescent and adult CF sputum levels ([33](#), [34](#)). Our analysis provides novel evidence that nanomolar NE activity is common in infants with CF and progressively increases with age despite best practice care. Given the pleiotropic effects of NE on biological systems, an increasing impact on epithelial homeostasis during childhood is likely.

Adhesion of epithelial cells to the extracellular matrix (ECM) structure and neighbouring cells is critical to maintaining epithelial barrier integrity. Free NE is able to digest a wide range of ECM molecules and our study found 100 nM NE activity reduced both attachment and viability in both pAEC_{non-CF} and pAEC_{CF} phenotypes. Exposure to NE significantly reduced monolayer confluence by 12 hours and less than 40% of cells remained attached by 48 hours. Cellular detachment in response to NE exposure has been reported elsewhere ([12](#)) however in that study, 80% detachment of A549 cells was only induced by 10 µg/mL (339 nM) NE, a concentration three-fold higher than required here for 80% detachment of pAEC ([12](#)). In addition, two other studies have described detachment of 16HBE14o⁻ or BET-1A cell lines by 100 nM NE but detachment was not quantified ([11](#), [14](#)). Others have reported no disruption to monolayers of primary human tracheal epithelial cells by concentrations of NE lower than 10 µg/mL ([20](#)), or not assessed NE concentrations similar to our study ([13](#), [17](#)). Overall, our investigation illustrated that pAEC from young airways demonstrate an increased sensitivity to NE activity compared to these adult cells investigated elsewhere.

Apoptosis was also induced when pAEC were exposed to NE. This agrees with previous data ([16-18](#)), where approximately two-fold increases in apoptosis were observed in epithelial cells after four hours exposure to NE. A proposed mechanism is proteolytic activation of proteinase-associated receptor-1 (PAR-1), triggering the caspase-9 apoptotic pathway ([16](#),

18). Interestingly, our data reported the apoptotic response by pAEC_{CF} to NE plateaued at 6 hours and was dampened in comparison to the response by pAEC_{non-CF}, which peaked at 12 hours post-exposure. Dampened apoptotic responses to viral infection by pAEC_{CF} have been reported previously by our group (27), suggesting reduced apoptotic responses are inherent to CF and may have important implications for CF respiratory disease, such as increased damage and an excessive pro-inflammatory response by the epithelium following insults. However, viral induction of apoptosis was not assessed in this study and future studies comparing both viral and protease induced apoptosis, whilst employing a wider array of apoptosis assays, may identify the defects in CF apoptotic pathways. After 48 hours exposure to NE, a small but significant increase in pAEC_{non-CF} supernatant levels of LDH was observed with a similar but non-significant trend in pAEC_{CF} supernatant. Whether increased cytotoxicity is due to the long exposure to NE is not known, since the one previous study in the literature that measured cytotoxicity only assessed a 30 minute exposure and found no increase in LDH (19). However, future time-course studies comparing apoptotic and cytotoxic responses could be informative on how persistent free NE activity in airways contributes to the CF inflammatory cycle through these processes (35). Overall, our data supports the concept that development of free NE activity initially drives an apoptotic, rather than necrotic, response in pediatric airway epithelium.

A pro-inflammatory response to 100 nM NE resulted in significantly increased IL-8 production by pAEC from healthy and CF cohorts, with a similar trend observed for IL-6. There are a number of studies that report NE concentrations as low as 10 nM inducing IL-8 production in both adult primary (21, 22) and epithelial cell lines (10, 11, 14). The lack of concordance at lower concentrations between the data presented here and the literature could be due to certain studies assessing cytokine mRNA rather than protein (12). In addition, the

longer exposure of 48 hours in our study could have led to IL-8 degradation by NE, as 1 $\mu\text{g/mL}$ (33.9 nM) NE has been shown to degrade IL-8 over 24 hours via proteolysis (36).

The most evident dose dependent effect of NE was on pAEC proliferation, with 100 nM NE significantly preventing proliferation when measured by either total or viable final cell number. Although cellular detachment by 100 nM NE is a possible confounder when interpreting viable cell number data, the measured lack of increase in final cell number from the initial seeding amount, as well as an accompanying lack of increase in monolayer confluence, corroborates our experimental interpretation that cellular proliferation could be reduced in airways with free NE activity. Inhibiting proliferation *in vivo* would limit the pool of cells available for epithelial homeostasis, repair and tissue turnover. Previous studies assessing NE and airway cell proliferation have been restricted to cell lines, with one study demonstrating cell cycle inhibition of NHBE's (37) whilst elsewhere ≥ 40 nM NE activity increased both 3H uptake and cell counts of the A549 cell line (38). Conflicting data in the literature may be due to biological differences, since in our study NE inhibited pAEC proliferation but had no observable effect on NuLi-1 or CuFi-1 proliferation. Altered cellular metabolism and increased resistance to NE-dependent cellular detachment by cell lines may explain their failure to recapitulate the pAEC data presented here.

Few studies have assessed airway cell wound repair in the presence of NE. One study reported that 0.03 Units/mL NE (20 nM NE) or greater inhibited wound closure of the cell line 16HBE14o⁻ by approximately 50% at 13 hours (19). Another study observed no inhibition of repair by the functionally related, keratinocyte skin epithelial cell after 9 hours incubation with 34 nM NE (39). Both of these studies only assessed wound closure at a single

time point. In contrast, our study assessed wound repair over 72 hours and data supported our hypothesis that nanomolar concentrations of NE can reduce epithelial repair. Incubation with 50 nM free NE activity significantly delayed pAEC_{CF} repair, although wound closure was completed by 72 hours. However, 100 nM completely abolished repair due to the significant detachment that occurred by 12 hours. Together, these findings suggest that free NE might prevent effective epithelial repair responses following injury *in vivo* and further implies a mechanistic role for NE in the formation of structural lung disease. Whether the effect over extended periods are due to NE exposure itself or a possible secondary effect induced by the original insult, is currently unknown and requires further investigation.

A novel and important critical finding from our study is that inhibited pAEC_{CF} repair could be rescued by inhibition of NE activity following initial exposure. Addition of α 1AT, even after 12 hours exposure to 50 nM NE that was enough to significantly delay repair, restored wound closure by pAEC_{CF} to control levels by 30 hours. Also reversed by α 1AT was the loss of adhesion due to 100 nM NE, resulting in reattachment and significantly increased wound closure by 72 hours. Although inhibition of NE has not been investigated in the context of pAEC repair, other studies have demonstrated that proteolytic-associated detachment of cells can be inhibited by protease inhibitors α 1AT, SLPI and elafin ([40](#), [41](#)), indicating that inhibiting proteolytic activity of NE should be the therapeutic aim. Our study assessed α 1AT as it is the major host antiprotease and is a therapy with a long track record, having been employed in various formats since 1988 to treat individuals with α 1AT deficiency ([42](#)). More recently, α 1AT received orphan drug designation for use as an aerosol therapy in adults with CF following several promising pre-clinical trials on deposition and protease inhibition ([33](#), [43](#), [44](#)). From the results presented here we speculate that targeted inhibition of free NE activity in very early CF disease may have a rapid and significant positive effect on epithelial

homeostasis. Synthetic inhibitors of NE are now available e.g., Sivelestat and AZD9668 that also possess potential for use in CF, although Sivelestat is only approved in Japan for clinical use in acute lung injury and clinical trial data reported limited efficacy for AZD6998 in COPD ([45](#), [46](#)).

Recent findings are now highlighting additional pathways through which uncontrolled NE activity can induce lung damage in CF, in particular the dysregulation of MMP activity by NE ([2](#), [47](#)). Dysregulated MMP-9 activity is associated with deficient wound repair, further mucous hypersecretion and airway remodelling in many airway diseases including CF ([48](#)) and excess MMP-1 and MMP-12 activation by NE can lead to α 1AT degradation that may prolong the cycle of excess NE activity and destruction ([49](#)). Therefore, chronic activation of these powerful modifiers of tissues and extracellular matrix by NE may be equally important to CF disease. Currently there are no MMP inhibitors approved and thus inhibiting upstream NE activity may present the most direct therapy available to prevent protease driven lung damage. To address these hypotheses, future studies are planned to address the relationship between NE and MMPs during repair of pAEC *in vitro* and the early stages of *in vivo* CF lung disease.

In summary, our data supported our hypotheses and suggest that free NE activity is deleterious for epithelial homeostasis, reducing adhesion and increasing apoptosis with an accompanying pro-inflammatory stimulation. Restoration of the airway epithelium during CF disease may also be restricted by NE. Thus, free NE is able to induce multiple cellular responses in the epithelium that could contribute to CF respiratory disease during early life. Studies using chest CT have identified a strong link between bronchiectasis and free NE

activity in infancy ([1](#), [5](#)) and observations reported here at NE concentrations lower than what can be detected in the paediatric CF airway, are consistent with protease activity in the airway contributing directly to CF structural lung disease. Therefore, a logical consideration is for clinical trials of antiprotease therapies in very young children with CF.

Acknowledgements:

The authors would like to thank Shyan Vijayasekaran, Paul Swan, Anthony Stroud, Ricardo Bergesio and Bernard Lee (St. John of God Hospital, Subiaco, Australia) for their assistance in collecting healthy control airway samples, Luke Berry (Telethon Kids Institute) for his technical assistance in processing BALf and the IL-8 and NE assays, as well as Peter Sly (Queensland Children's Medical Research Institute, Brisbane, Australia) and Andre Schultz (Princess Margaret Hospital for Children) for their comments during manuscript preparation. AREST CF would like to thank the contributions of respiratory fellows and nurses at Princess Margaret Hospital for Children, Telethon Kids Institute, Royal Children's Hospital Melbourne and Murdoch Children's Research Institute. We would also like to thank the participants and their families who took part in the study.

References:

1. Stick SM, Brennan S, Murray C, Douglas T, von Ungern-Sternberg BS, Garratt LW, Gangell CL, De Klerk N, Linnane B, Ranganathan S, et al. Bronchiectasis in infants and preschool children diagnosed with cystic fibrosis after newborn screening. *J Pediatr* 2009;155(5):623-628.e621.
2. Gaggar A, Li Y, Weathington N, Winkler M, Kong M, Jackson P, Blalock JE, Clancy JP. Matrix metalloprotease-9 dysregulation in lower airway secretions of cystic fibrosis patients. *Am J Physiol Lung Cell Mol Physiol* 2007;293(1):L96-L104.
3. Birrer P, McElvaney NG, Rudeberg A, Sommer CW, Liechti-Gallati S, Kraemer R, Hubbard R, Crystal RG. Protease-antiprotease imbalance in the lungs of children with cystic fibrosis. *Am J Respir Crit Care Med* 1994;150(1):207-213.
4. Khan TZ, Wagener JS, Bost T, Martinez J, Accurso FJ, Riches DW. Early pulmonary inflammation in infants with cystic fibrosis. *Am J Respir Crit Care Med* 1995;151(4):1075-1082.
5. Sly PD, Gangell CL, Chen L, Ware RS, Ranganathan S, Mott LS, Murray CP, Stick SM, Investigators AC. Risk factors for bronchiectasis in children with cystic fibrosis. *N Engl J Med* 2013;368(21):1963-1970.
6. Mott LS, Park J, Murray CP, Gangell CL, de Klerk NH, Robinson PJ, Robertson CF, Ranganathan SC, Sly PD, Stick SM. Progression of early structural lung disease in young children with cystic fibrosis assessed using ct. *Thorax* 2012;67(6):509-516.
7. Lungarella G, Cavarra E, Lucattelli M, Martorana PA. The dual role of neutrophil elastase in lung destruction and repair. *Int J Biochem Cell Biol* 2008;40(6-7):1287-1296.
8. Connett GJ. Bronchoalveolar lavage. *Paediatr Respir Rev* 2000;1(1):52-56.
9. Piorunek T, Marszalek A, Biczysko W, Gozdzik J, Cofta S, Seget M. Correlation between the stage of cystic fibrosis and the level of morphological changes in adult patients. *J Physiol Pharmacol* 2008;59 Suppl 6:565-572.
10. Nakamura H, Yoshimura K, McElvaney NG, Crystal RG. Neutrophil elastase in respiratory epithelial lining fluid of individuals with cystic fibrosis induces interleukin-8 gene expression in a human bronchial epithelial cell line. *J Clin Invest* 1992;89(5):1478-1484.
11. Shibata Y, Nakamura H, Kato S, Tomoike H. Cellular detachment and deformation induce il-8 gene expression in human bronchial epithelial cells. *J Immunol* 1996;156(2):772-777.
12. Van Wetering S, Mannesse-Lazeroms SP, Dijkman JH, Hiemstra PS. Effect of neutrophil serine proteinases and defensins on lung epithelial cells: Modulation of cytotoxicity and il-8 production. *J Leukoc Biol* 1997;62(2):217-226.
13. Hashimoto S, Maruoka S, Gon Y, Matsumoto K, Takeshita I, Horie T. Mitogen-activated protein kinase involves neutrophil elastase-induced morphological changes in human bronchial epithelial cells. *Life Sci* 1999;64(16):1465-1471.
14. Walsh DE, Greene CM, Carroll TP, Taggart CC, Gallagher PM, O'Neill SJ, McElvaney NG. Interleukin-8 up-regulation by neutrophil elastase is mediated by myd88/irak/traf-6 in human bronchial epithelium. *J Biol Chem* 2001;276(38):35494-35499.
15. Liu C-Y, Liu Y-H, Lin S-M, Yu C-T, Wang C-H, Lin H-C, Lin C-H, Kuo H-P. Apoptotic neutrophils undergoing secondary necrosis induce human lung epithelial cell detachment. *J Biomed Sci* 2003;10(6 Pt 2):746-756.
16. Suzuki T, Moraes TJ, Vachon E, Ginzberg HH, Huang T-T, Matthay Ma, Hollenberg MD, Marshall J, McCulloch CaG, Abreu MTH, et al. Proteinase-activated receptor-1

mediates elastase-induced apoptosis of human lung epithelial cells. *Am J Respir Cell Mol Biol* 2005;33(3):231-247.

17. Song JS, Kang CM, Rhee CK, Yoon HK, Kim YK, Moon HS, Park SH. Effects of elastase inhibitor on the epithelial cell apoptosis in bleomycin-induced pulmonary fibrosis. *Exp Lung Res* 2009;35(10):817-829.

18. Suzuki T, Yamashita C, Zemans RL, Briones N, Van Linden A, Downey GP. Leukocyte elastase induces lung epithelial apoptosis via a par-1-, nf-kappab-, and p53-dependent pathway. *Am J Respir Cell Mol Biol* 2009;41(6):742-755.

19. Ewen D, Clarke SL, Smith JR, Berger C, Salmon G, Trevethick M, Shute JK. The role of protease-activated receptors par-1 and par-2 in the repair of 16hbe 14o(-) epithelial cell monolayers in vitro. *Clin Exp Allergy* 2010;40(3):435-449.

20. Kerckmar CM, Davis PB. Resistance of human tracheal epithelial cells to killing by neutrophils, neutrophil elastase, and pseudomonas elastase. *Am J Respir Cell Mol Biol* 1993;8(1):56-62.

21. Bédard M, McClure CD, Schiller NL, Francoeur C, Cantin A, Denis M. Release of interleukin-8, interleukin-6, and colony-stimulating factors by upper airway epithelial cells: Implications for cystic fibrosis. *Am J Respir Cell Mol Biol* 1993;9(4):455-462.

22. Witherden IR, Vanden Bon EJ, Goldstraw P, Ratcliffe C, Pastorino U, Tetley TD. Primary human alveolar type ii epithelial cell chemokine release: Effects of cigarette smoke and neutrophil elastase. *Am J Respir Cell Mol Biol* 2004;30(4):500-509.

23. Garratt LW, Sutanto EN, Foo CJ, Ling KM, Looi K, Kicic-Starceвич E, Iosifidis T, Martinovich KM, Lannigan FJ, Stick SM, et al. Determinants of culture success in an airway epithelium sampling program of young children with cystic fibrosis. *Exp Lung Res* 2014;40(9):447-459.

24. Looi K, Sutanto EN, Banerjee B, Garratt L, Ling K-M, Foo CJ, Stick SM, Kicic A. Bronchial brushings for investigating airway inflammation and remodelling. *Respirology* 2011;16(5):725-737.

25. Kicic A, Sutanto EN, Stevens PT, Knight DA, Stick SM. Intrinsic biochemical and functional differences in bronchial epithelial cells of children with asthma. *Am J Respir Crit Care Med* 2006;174(10):1110-1118.

26. Kicic A, Hallstrand TS, Sutanto EN, Stevens PT, Kobor MS, Taplin C, Paré PD, Beyer RP, Stick SM, Knight DA. Decreased fibronectin production significantly contributes to dysregulated repair of asthmatic epithelium. *Am J Respir Crit Care Med* 2010;181(9):889-898.

27. Sutanto EN, Kicic A, Foo CJ, Stevens PT, Mullane D, Knight DA, Stick SM. Innate inflammatory responses of pediatric cystic fibrosis airway epithelial cells: Effects of nonviral and viral stimulation. *Am J Respir Cell Mol Biol* 2011;44(6):761-767.

28. Garratt LW, Sutanto EN, Ling K-M, Looi K, Kicic-Starceвич E, Iosifidis T, Martinovich KM, Lannigan FJ, Stick SM, Kicic A, et al. Alpha 1-antitrypsin mitigates neutrophil elastase inhibition of airway epithelial wound repair in children with cystic fibrosis. *Respirology* 2014;19(Supplement S2):32-34.

29. Garratt LW, Sutanto EN, Ling K-M, Looi K, Kicic-Starceвич E, Iosifidis T, Martinovich KM, Lannigan FJ, Stick SM, Kicic A, et al. Alpha-1 antitrypsin ameliorates inhibition of wound repair by neutrophil elastase. *Eur Respir J* 2014;44(Suppl. 58):3467-3467.

30. Berry LJ, Sheil B, Garratt L, Sly PD. Stability of interleukin 8 and neutrophil elastase in bronchoalveolar lavage fluid following long-term storage. *J Cyst Fibros* 2010;9(5):346-350.

31. Sundaram GM, Common JEA, Gopal FE, Srikanta S, Lakshman K, Lunny DP, Lim TC, Tanavde V, Lane EB, Sampath P. 'See-saw' expression of microRNA-198 and fstl1 from a single transcript in wound healing. *Nature* 2013;495(7439):103-106.
32. Armstrong DS, Grimwood K, Carlin JB, Carzino R, Gutiérrez JP, Hull J, Olinsky A, Phelan EM, Robertson CF, Phelan PD. Lower airway inflammation in infants and young children with cystic fibrosis. *Am J Respir Crit Care Med* 1997;156(4):1197-1204.
33. Cantin AM, Berthiaume Y, Cloutier D, Martel M. Prolastin aerosol therapy and sputum taurine in cystic fibrosis. *Clinical and investigative medicine Médecine clinique et expérimentale* 2006;29(4):201-207.
34. Mayer-Hamblett N, Aitken ML, Accurso FJ, Kronmal RA, Konstan MW, Burns JL, Sagel SD, Ramsey BW. Association between pulmonary function and sputum biomarkers in cystic fibrosis. *Am J Respir Crit Care Med* 2007;175(8):822-828.
35. Vandivier RW, Henson PM, Douglas IS. Burying the dead: The impact of failed apoptotic cell removal (efferocytosis) on chronic inflammatory lung disease. *Chest* 2006;129(6):1673-1682.
36. Leavell KJ, Peterson MW, Gross TJ. Human neutrophil elastase abolishes interleukin-8 chemotactic activity. *J Leukoc Biol* 1997;61(3):361-366.
37. Fischer BM, Zheng S, Fan R, Voynow JA. Neutrophil elastase inhibition of cell cycle progression in airway epithelial cells in vitro is mediated by p27kip1. *Am J Physiol Lung Cell Mol Physiol* 2007;293(3):L762-L768.
38. Houghton AM, Rzymkiewicz DM, Ji H, Gregory AD, Egea EE, Metz HE, Stolz DB, Land SR, Marconcini LA, Kliment CR, et al. Neutrophil elastase-mediated degradation of irs-1 accelerates lung tumor growth. *Nat Med* 2010;16(2):219-223.
39. Buchstein N, Hoffmann D, Smola H, Lang S, Paulsson M, Niemann C, Krieg T, Eming SA. Alternative proteolytic processing of hepatocyte growth factor during wound repair. *Am J Pathol* 2009;174(6):2116-2128.
40. Li Q, Zhou XD, Xu XY, Yang J. Recombinant human elafin protects airway epithelium integrity during inflammation. *Mol Biol Rep* 2010;37(6):2981-2988.
41. Bingle L, Richards RJ, Fox B, Masek L, Guz A, Tetley TD. Susceptibility of lung epithelium to neutrophil elastase: Protection by native inhibitors. *Mediators Inflamm* 1997;6(5-6):345-354.
42. Karnaukhova E. Recent advances in the research and development of alpha-1 proteinase inhibitor for therapeutic use. In: Irusen EM, editor. Lung diseases - selected state of the art reviews. Rijeka: InTech;2012. p. 83-104.
43. Griese M, Latzin P, Kappler M, Weckerle K, Heinzlmaier T, Bernhardt T, Hartl D. Alpha1-antitrypsin inhalation reduces airway inflammation in cystic fibrosis patients. *Eur Respir J* 2007;29(2):240-250.
44. Brand P, Schulte M, Wencker M, Herpich CH, Klein G, Hanna K, Meyer T. Lung deposition of inhaled alpha1-proteinase inhibitor in cystic fibrosis and alpha1-antitrypsin deficiency. *Eur Respir J* 2009;34(2):354-360.
45. Elborn JS, Perrett J, Forsman-Semb K, Marks-Konczalik J, Gunawardena K, Entwistle N. Efficacy, safety and effect on biomarkers of azd9668 in cystic fibrosis. *Eur Respir J* 2012;40(4):969-976.
46. Vogelmeier C, Aquino TO, O'Brien CD, Perrett J, Gunawardena KA. A randomised, placebo-controlled, dose-finding study of azd9668, an oral inhibitor of neutrophil elastase, in patients with chronic obstructive pulmonary disease treated with tiotropium. *COPD* 2012;9(2):111-120.
47. Jackson PL, Xu X, Wilson L, Weathington NM, Clancy JP, Blalock JE, Gaggar A. Human neutrophil elastase-mediated cleavage sites of mmp-9 and timp-1: Implications to cystic fibrosis proteolytic dysfunction. *Mol Med* 2010;16(5-6):159-166.

48. Gaggar A, Hector A, Bratcher PE, Mall MA, Griese M, Hartl D. The role of matrix metalloproteinases in cystic fibrosis lung disease. *Eur Respir J* 2011;38(3):721-727.
49. Shapiro SD, Goldstein NM, Houghton AM, Kobayashi DK, Kelley D, Belaaouaj A. Neutrophil elastase contributes to cigarette smoke-induced emphysema in mice. *Am J Pathol* 2003;163(6):2329-2335.

Figure 1: Effect of free NE on confluence and viability in pAECs. Monolayer cultures of pAEC were exposed to NE over 48 hours and then cell confluence, viability and cytotoxicity assessed. No change in confluence by pAEC_{non-CF} (A) and pAEC_{CF} (B) was observed for control media (circles), 10 nM (squares) or 50 nM (triangles) NE over 48 hours. In contrast, 100 nM NE (diamonds) significantly reduced monolayer confluence as early as 12 hours. Assessment of cellular viability by MTS assay (C) demonstrated that cell number of both pAEC_{non-CF} (open bars) and pAEC_{CF} (closed bars) was significantly decreased in response to 100 nM NE, compared to respective controls. LDH production represented as a fold change over untreated (D) was significantly induced in pAEC_{non-CF} (open bars) by 100 nM NE, but did not reach significance for pAEC_{CF} (closed bars). Data was obtained from four to eight separate experiments, with each point in duplicate. *Indicates $p < 0.05$ for 100 nM NE.

Figure 2: Effect of free NE on apoptotic induction and inflammatory cytokine production in pAEC. Monolayer cultures of pAEC_{non-CF} (A) and pAEC_{CF} (B) were exposed to 10 nM (squares), 50 nM (triangles) and 100 nM (diamonds) NE over 48 hours and apoptosis assessed at 3, 6, 12, 24 and 48 hours by ssDNA formation. Results were then represented as a fold change over control media. Exposure of pAEC_{non-CF} to 100 nM NE significantly induced apoptosis as early as three hours and this remained significantly higher by 24 hours (A). Apoptosis was also seen in pAEC_{CF} exposed to 100 nM NE, although this was only significant at 6 hours (B). No significant change was observed for either 10 or 50 nM NE. Supernatants were also assessed by ELISA to measure IL-6 (C) and IL-8 production (D). IL-6 production was significantly higher in pAEC_{CF} (closed bars) treated with 100 nM NE, while IL-8 production was significantly higher for both pAEC_{non-CF} (open bars) and

pAEC_{CF} (closed bars). Data was obtained from four to eight separate experiments, with each point in duplicate. *Indicates $p < 0.05$ for 100 nM NE.

Figure 3: Effect of free NE on cell proliferation in pAECs. pAEC were seeded at 5,000 cells/well and incubated for 24 hours to facilitate attachment. Cells were then exposed to NE over 120 hours and proliferation was assessed. Confluence of pAEC_{non-CF} (A) and pAEC_{CF} (B) increased in response to both control media (circles) and 10 nM NE (squares). However, confluence remained static or decreased in the presence of 50 nM (triangles) and 100 (diamonds) nM NE respectively. After 120 hours, cell number was determined through cell counting of time-lapse images (C). Final cell number of pAEC_{non-CF} (open bars) and pAEC_{CF} (closed bars) was significantly lower for 100 nM NE compared to control media. Subsequent assessment of cell viability by MTS (D) demonstrated 50 nM and 100 nM NE significantly reduced final viable cell number of pAEC_{non-CF} (open bars) and pAEC_{CF} (closed bars) in comparison to control media. Data was obtained from four separate experiments, with each point performed in quadruplicate. *Indicates $p < 0.05$ to control.

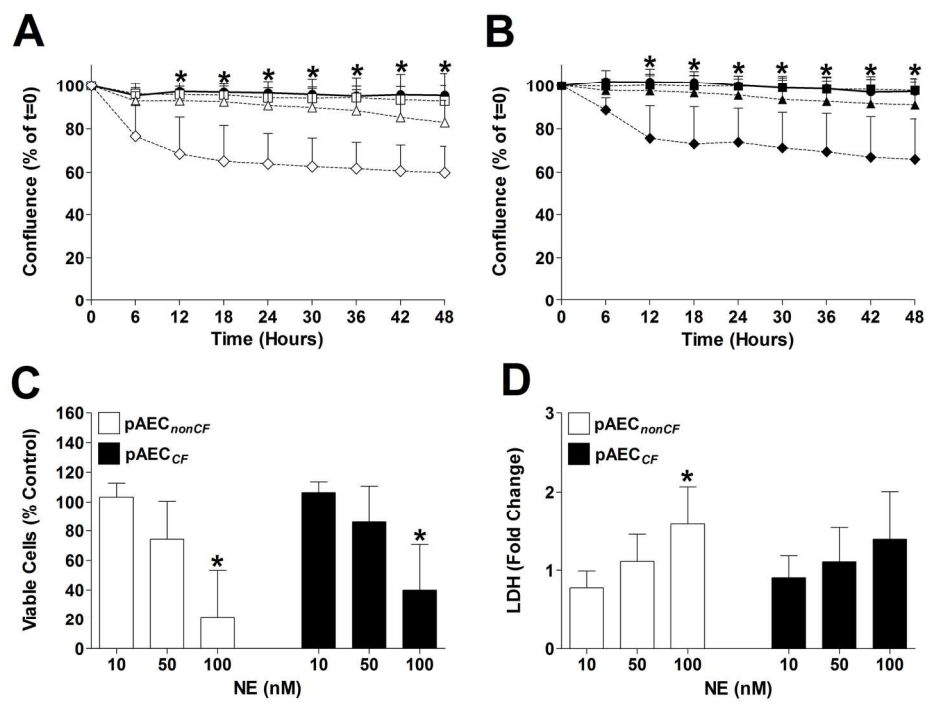
Figure 4: Effect of free NE on pAEC_{CF} wound repair. Confluent pAEC_{CF} monolayer cultures were scratch wounded and repair in the presence of NE observed and quantified. In control media (circles) and 10 nM NE (squares), pAEC_{CF} achieved 85% closure by 30 hours post wounding and 100% by 54 hours. However, 50 nM NE (triangles) significantly reduced wound closure at 30 hours. A more pronounced effect on repair was observed for 100 nM NE (diamonds), with significantly reduced wound closure observed at 12 hours that remained over 72 hours. *Indicates $p < 0.05$ to control media, dotted line represents mean closure of

pAEC_{CF} at 30 hours in control media. Data was collated from five separate experiments, with each point performed in triplicate.

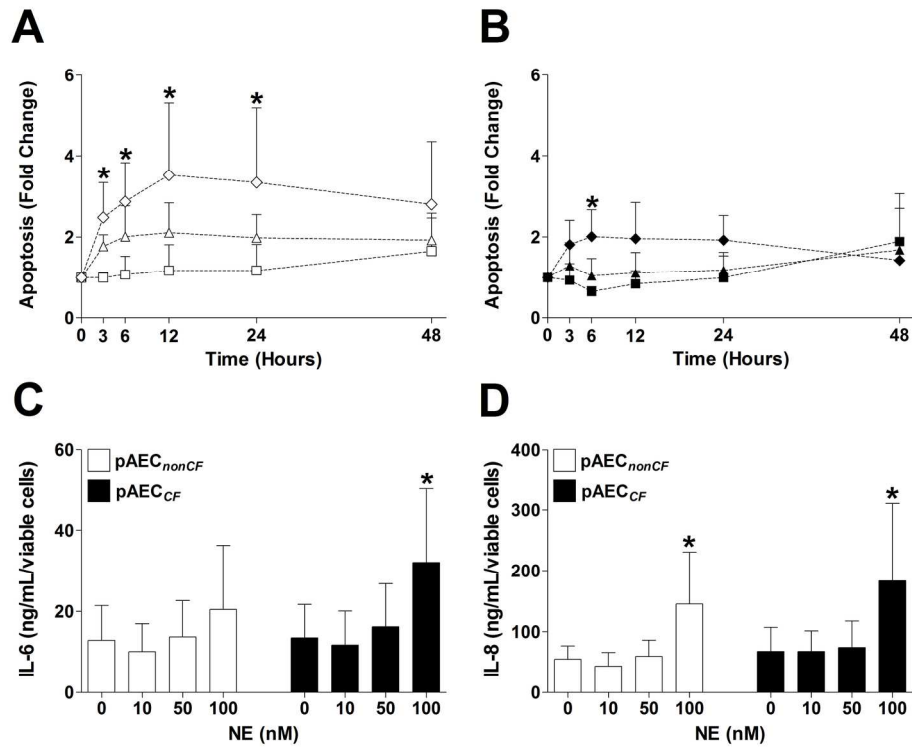
Figure 5: Effects of α 1AT on NE inhibited pAEC_{CF} wound repair. (A) Confluent monolayer cultures of pAEC_{CF} were scratch wounded and repair observed in the presence of α 1AT (half closed circles). No significant difference in wound repair by pAEC_{CF} in control media (closed circles) was seen following addition of 1 μ M α 1AT (half closed circles). (B) Repair of scratch wounded cultures was also assessed in the presence of 50 nM (closed triangles) and 100 nM NE (closed diamonds). At 12 hours post wounding, 1 μ M α 1AT was added to a number of wells to inhibit free NE (50 nM and 100 nM NE). Treatment of pAEC_{CF} exposed to 50 nM NE with α 1AT (half closed triangles) significantly improved wound closure at 30 hours to levels and were similar to controls. Furthermore, repair of pAEC_{CF} exposed to 100 nM NE and α 1AT (half closed diamonds) was also significantly increased by 30 hours and closure continued through to 72 hours. *Indicates $p < 0.05$ to NE without α 1AT treatment, dotted line represents mean closure of pAEC_{CF} at 30 hours in control media. Data was collated from five separate experiments, with each point performed in triplicate.

Figure 6: Effect of α 1AT treatment on viable cell number. Confluent monolayer cultures of pAEC_{CF} were scratch wounded and repair in the presence of NE observed. At 12 hours post wounding, 1 μ M α 1AT was added to a number of wells to inhibit NE. After a further 72 hours, viability of pAEC_{CF} exposed to NE alone (closed bars) and pAEC_{CF} treated with α 1AT at 12 hours (striped bars) was measured by MTS assay. Exposure of cells to 100 nM NE significantly reduced viable cell number, but this was significantly increased by α 1AT treatment. However, viable cell number remained significantly lower than control. *Indicates

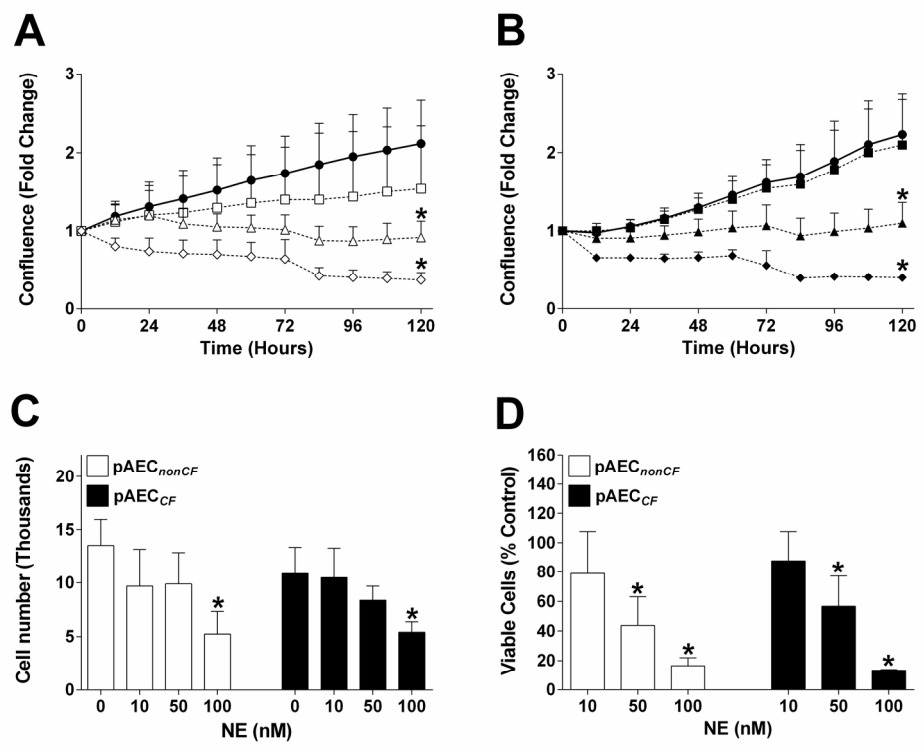
p<0.05 to control, # indicates p<0.05 to 100 nM NE alone. Data was collated from five separate experiments, with each point performed in triplicate.



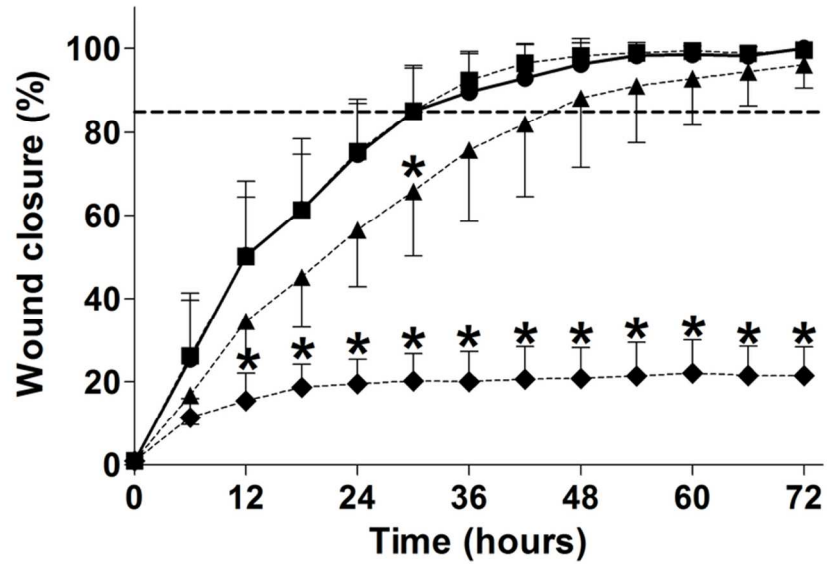
170x127mm (300 x 300 DPI)



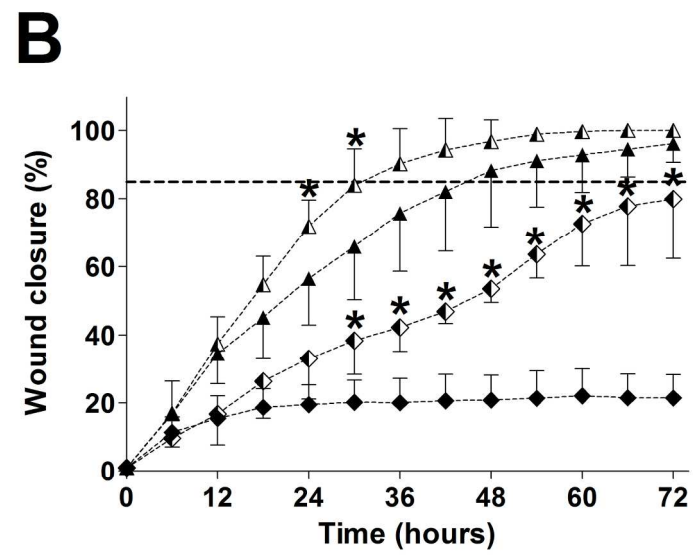
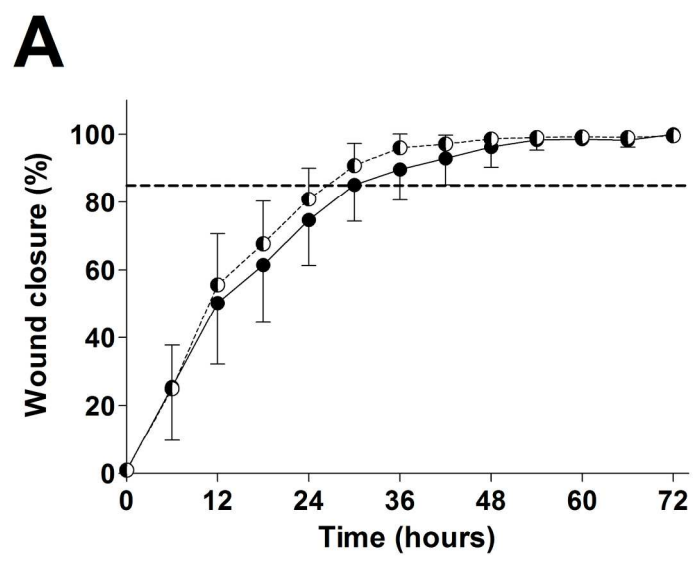
181x145mm (300 x 300 DPI)



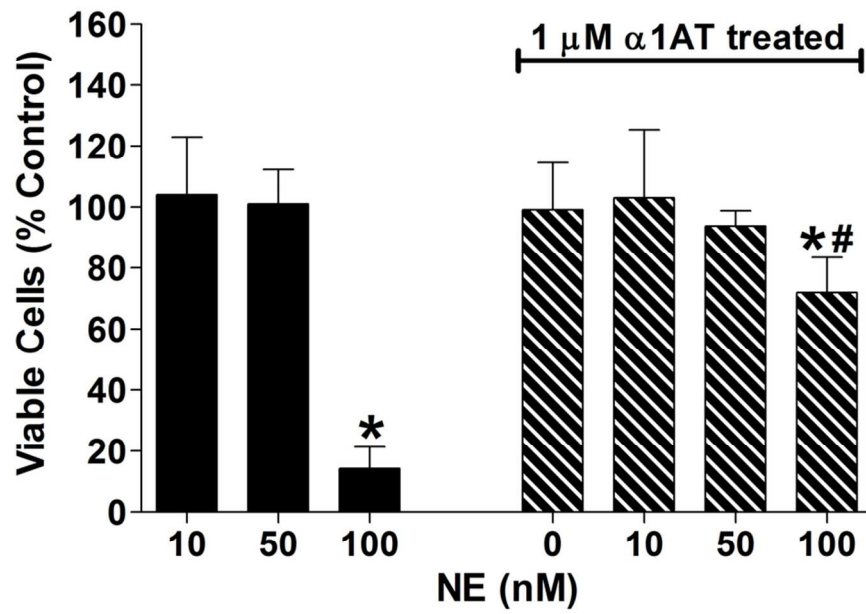
184x146mm (300 x 300 DPI)



83x57mm (300 x 300 DPI)



174x252mm (300 x 300 DPI)



92x62mm (300 x 300 DPI)

ONLINE DATA SUPPLEMENT

Alpha 1-antitrypsin mitigates the inhibition of airway epithelial cell repair by neutrophil elastase

Luke W Garratt, Erika N Sutanto, Kak-Ming Ling, Kevin Looi, Thomas Iosifidis, Kelly M Martinovich, Nicole C Shaw, Alysia G Buckley, Elizabeth Kicic-Starceвич, Francis J Lannigan, Darryl A Knight, Stephen M Stick & Anthony Kicic on behalf of AREST CF

MATERIALS AND METHODS:

Reagents

The following reagents were sourced for this study. Bovine pituitary extract, recombinant human epidermal growth factor, epinephrine hydrochloride, hydrocortisone, insulin, methanol, N-methyl-2-pyrrolidone, N-methoxysuccinyl Ala-Ala-Pro-Val p-nitroanilide, all trans retinoic acid, transferrin, triiodothyronine, Trizma base, Trizma hydrochloride and trypsin were purchased from Sigma-Aldrich (St Louis, MO, USA). Amphotericin B, fetal bovine serum (FBS), gentamicin, penicillin/streptomycin and RPMI-1640 media were purchased from Invitrogen (Melbourne, Victoria, Australia). Collagens S (type I) as well as fibronectin were purchased from Roche (Sydney, New South Wales, Australia). Bronchial epithelial basal medium (BEBM) was purchased from Lonza (Basel, Switzerland). Ultrosor G was purchased from Pall Biosepra (Cergy-Saint Christophe, France). All plasticware was purchased from In Vitro Technologies (Melbourne, Victoria, Australia), except for 96 well Essen ImageLock plates from Millenium Science (Melbourne, Victoria, Australia). Purified human sputum neutrophil elastase (NE) for *in vitro* cell exposure was purchased from Elastin Products Company (Owensville, MO, USA), purified human blood NE for the assessment of NE activity in BALf as previously described (E1, E2) was purchased from Calbiochem

(Darmstadt, Germany). Purified human plasma alpha-1 antitrypsin was purchased Athens Research Technology (Athens, GA, USA).

Cell culture

Primary cultures were plated into tissue culture vessels pre-coated with fibronectin (10mM), collagen (30mM) and bovine serum albumin (100mM) and expanded unmodified as previous described (E2, E3). Bronchial epithelial growth medium (BEGM) was used for all cell culture and consisted of bronchial epithelial basal medium (BEBM), supplemented with 50 µg/ml bovine pituitary extract, 25 ng/ml recombinant human epidermal growth factor (EGF), 0.5 µg/ml epinephrine hydrochloride, 0.5 µg/ml hydrocortisone, 5 µg/ml insulin, 0.1 ng/ml all trans retinoic acid, 10 µg/ml transferrin and 6.5 ng/ml triiodothyronine, 0.125 µg/ml amphotericin B, 50 µg/ml gentamicin, penicillin/streptomycin (10 Units/mL penicillin and 0.01 mg/mL streptomycin) and 2% (v/v) Ultrosor G. Established cultures were fed every second day and were passaged every 14-21 days with 0.25% Trypsin/0.05% EDTA, with experimental assays performed at passages one or two.

NuLi-1 and CuFi-1 cells (CRL-4011 and CRL-4013, ATCC, Manassas, VA, USA) are bronchial epithelial cells derived from normal and CF human lung respectively, transformed using human telomerase reverse transcriptase (hTERT) and human papillomavirus type 16 E6 and E7 genes (E4). Bronchial epithelial growth medium (BEGM) was used for all cell culture and tissue culture vessels were pre-coated with fibronectin (10mM), collagen (30mM) and bovine serum albumin (100mM). Established cultures were fed every second day and were passaged every 5-7 days with 0.25% Trypsin/0.05% EDTA, with experimental assays performed between passages four and nine.

Assessment of viability

Cell viability and proliferation was evaluated using the CellTiter 96 MTS (3-(4,5-dimethylthiazol-2-yl)-5-(3-carboxymethoxyphenyl)-2-(4-sulfophenyl)-2H-tetrazolium inner salt) assay, which is based on the reduction of the tetrazolium salt to a formazan product by mitochondrial dehydrogenases of living cells (Promega, WI, USA) (E5). Results were interpreted as formazan product formation compared to controls.

To evaluate the effect of NE on epithelial monolayers, cell cultures were maintained in BEGM on 96-well microtitre plate until >95% confluent. A dose range of 0 nM to 100 nM NE was made in 200 μ L EGF-free BEGM with 0.5% (v/v) UG and incubated over 48 hours at 37°C. Phase contrast time-lapse images were taken every two hours using an IncuCyte live-cell imaging system (Essen Bioscience, Ann Arbor, MI, USA). Cell supernatants were retained at the end of the experiment and stored at -80°C for down-stream assessment. Wells were washed once with serum-free clear RPMI-1640 before the MTS assay was performed in serum-free clear RPMI-1640 (E6). Plates were left to incubate for 2 hours at 37°C degrees and finally read on a Multiskan FC spectrophotometer (Thermo Fisher Scientific, Melbourne, VIC, Australia) at a wavelength of 490 nm.

To evaluate the effect of NE on epithelial proliferation, cells were seeded aseptically into a 96-well microtitre plate at a density of 5,000 cells per well and maintained overnight at 37°C to ensure attachment. This density was shown previously to yield an exponential growth phase of cells over a 5 day time period (data not shown). A dose range of 0 nM to 100 nM NE was made in 200 μ L EGF free BEGM with 0.5% (v/v) UG, and plates incubated over 5 days at 37°C. Phase contrast time-lapse images were taken every two hours using an IncuCyte live-cell imaging system (Essen Bioscience, Ann Arbor, MI, USA). After 3 days,

media was carefully refreshed by two thirds volume. After 5 days incubation, wells were washed once with serum-free clear RPMI-1640 before MTS assay was performed. In addition to viability assessment, proliferation was also measured as final total cell number, which was obtained by manual counting of cells in images taken at 120 hours.

Cell viability and proliferation results were complemented by assessment of cellular confluence, recorded through image analysis by the IncuCyte software (Essen Bioscience, Ann Arbor, MI, USA) and interpreted as a fold change from the first image.

Assessment of apoptosis

Apoptosis was assessed using a single-stranded DNA (ssDNA) apoptosis kit (Millipore, Billerica, MA, USA) as previously described (E3), which measures apoptotic cells through formamide denaturation and antibody detection of ssDNA (E7). Briefly, assays were performed in a 96-well microtitre with cells seeded at a density of 20,000 cells per well. A dose range of 0 nM to 100 nM NE was made in 200 μ L EGF free BEGM with 0.5% (v/v) UG, and plates incubated over 5 days at 37°C. At 3, 6, 12, 24 and 48 hours, supernatant was carefully collected to prevent cell removal before the monolayer was fixed at room temperature for 30 minutes with 200 μ L of 80% (v/v) methanol in PBS. Following fixation, plates were air-dried overnight in a laminar flow hood to ensure adherence of all cells. Formamide incubation denatured DNA in apoptotic cells only, permitting antibody binding of ssDNA that was subsequently quantified with plates read at a wavelength of 405 nm on a Multiskan FC spectrophotometer. A negative control was provided by DNase incubation to ensure antibody specificity, and a well coated with ssDNA used as positive control. Results were represented as fold change in signal over cells exposed to control media as directed by the manufacturer

Assessment of cytotoxicity

Cellular cytotoxicity was quantified via the CytoTox 96 colorimetric assay (Promega, Madison, WI, USA) as previously described (E3), which measures the amount of lactate dehydrogenase (LDH) release due to necrotic cell lysis. LDH is a large intracellular molecule which is unable to cross the cell membrane (E8). Briefly, stored supernatant from the viability and apoptosis experiments were thawed, mixed with CytoTox 96 Substrate Mix and incubated for 30 minutes at RT, protected from light. The enzymatic reaction was then stopped with CytoTox 96 Stop Solution and colour change was measured using a Multiskan FC spectrophotometer at 490 nm. Results were interpreted as a fold change from control.

Assessment of wound repair

The ability of airway epithelial cells to repair wounds following NE exposure was assessed by scratch wounding and image analysis, as described previously (E9). Briefly, pAEC_{CF} cultures were maintained in BEGM on 96 well ImageLock tissue culture plates until >95% confluent. Using a WoundMaker device (Essen Bioscience, Ann Arbor, MI, USA), monolayers were wounded with a single linear scratch twice in both directions and washed once with EGF free BEGM with 0.5% (v/v) UG. A dose range of 10 nM to 100 nM NE was made in 135 μ L EGF free BEGM with 0.5% (v/v) UG and added to appropriate wells. For experiments assessing wound repair in the presence of NE inhibited by 1 μ M α 1AT, 15 μ L of 10 μ M α 1AT was added 12 hours post wounding to achieve a final concentration of 1 μ M. Alternatively, 15 μ L of EGF free BEGM with 0.5% (v/v) UG was added as media control. Cultures were incubated at 37°C and scratch area was monitored using an IncuCyte live-cell

imaging system (Essen Bioscience, Ann Arbor, MI, USA), with wound closure calculated by identification of cellular confluence through image analysis and comparing to that of the originally created wound area. After 72 hours incubation, cell supernatants were retained at -80°C and the monolayer was washed once with serum-free clear RPMI 1640 before MTS assay was performed. Results were standardised as a percentage of control.

Assessment of bronchiectasis

Scans were scored for bronchiectasis with no prior knowledge of child's health using a modified Brodie score as previously described (E10). Bronchiectasis was then identified as a bronchus-to-artery ratio of more than one and scoring the extent in each lobe as zero, one or two for no observable bronchiectasis, <50% of visible airways and >50% visible airways respectively. The maximum score for a scan was 12.

Assessment of neutrophil elastase

Free NE activity was assessed using an quantitative adapted assay (E11) as previously described (E1, E2). Briefly, BAL fluid (BALf) supernatant was serially diluted 1:2 with 0.2 M Tris buffer pH 8 in duplicate. Tris buffer was also used as the negative control and to dilute the human neutrophil elastase standard, serially diluted from 25 µg/mL (847.5 nM) to 0.02 µg/mL (0.7 nM). Substrate N-methoxysuccinyl Ala-Ala-Pro-Val p-nitroanilide was dissolved in N-methyl-2-pyrrolidone to a final concentration of 100 mM, then added to each well. Free NE activity cleaves 4-nitroaniline from the substrate, increasing absorbance at 405 nM. Absorbance was read immediately after substrate addition and again after 20, 30 and 40 minutes incubation at 37°C. The time point with the best standard curve according to r-value,

typically 40 minutes, was taken to determine activity and results were calculated using AssayZap (Biosoft, Cambridge, UK). The lower limit of detection for this assay was 0.2 $\mu\text{g/mL}$ (6.8 nM). A sample from a separate subject with known elevated NE levels was used as an inter-assay positive control and the inter-assay coefficient of variation was previously established at 7.99% (E1).

Sample	Age (years)	Sex	CFTR Genotype	CFTR Class*	Neutrophil Elastase (nM)	Bronchiectasis (0 – 12) [†]	Respiratory Pathogens [‡]
1	4.25	F	p.Phe508del / p.Arg117His	2 / 4	N.D.	0	<i>Mixed oral flora, Staphylococcus aureus</i>
2	4.63	F	p.Phe508del / p.Ile336SerfsX28	2 / 1	N.D.	0	<i>Stenotrophomonas maltophilia</i>
3	4.45	F	p.Arg553X / c.1367T>C	1 / -	N.D.	0	N.D.
4	6.42	M	p.Phe508del / c.1585-1G>A	2 / 1	N.D.	2	N.D.
5	5.09	F	p.Phe508del / p.Gly27X	2 / 1	N.D.	1	<i>Stenotrophomonas maltophilia</i>
6	1.34	F	p.Phe508del / c.3367G	2 / -	N.D.	0	N.D.
7	1.97	M	p.Phe508del / Unknown	2 / -	N.D.	1	<i>Pseudomonas aeruginosa</i>
8	3.94	F	p.Phe508del / p.Gly551Asp	2 / 3	N.D.	0	N.D.
9	5.30	M	p.Phe508del / c.2657+2 3insA	2 / -	N.D.	0	N.D.
10	6.16	F	p.Phe508del / p.Arg347Pro	2 / 4	30.17	1	<i>Aspergillus flavus, Aspergillus fumigatus</i>
11	5.16	M	p.Phe508del / c.2657+5G>A	2 / 5	N.D.	1	N.D.
12	4.94	F	p.Phe508del / p.Gly551Asp	2 / 3	N.D.	1	N.D.
13	6.18	F	p.Phe508del / p.Lys447ArgfsX2	2 / -	411.86	1	N.D.
14	6.16	M	p.Phe508del / c.2657+5G>A	2 / 5	N.D.	2	N.D.
15	5.96	M	p.Phe508del / p.Arg117His	2 / 4	N.D.	0	<i>Haemophilus influenzae</i>
16	0.27	F	p.Phe508del / p.Phe508del	2 / 2	N.D.	0	N.D.

Supplementary Table 1. Demographics of subjects from which pAEC_{CF} were obtained. N.D. = none detected. *Only known classes reported, [†]bronchiectasis on CT scan scored blindly by clinical radiologist, [‡]pathogen data at time of brushing obtained from clinical assessment of BALf.

Age years	BALf n	Total Cohort		BALf with Detectable Free NE*	
		Mean NE <i>nM</i> ±SD	Maximum NE <i>nM</i>	BALf n (% total)	Mean Detected NE <i>nM</i> ±SD
0 – 1	232	20.24 ±63.70	728.17	70 (30.17%)	62.61 ±104.90
1 – 2	245	37.08 ±207.54	3,000.15	59 (24.08%)	146.38 ±406.49
2 – 3	202	32.06 ±101.78	1,050.90	63 (31.19%)	98.08 ±164.84
3 – 4	213	51.49 ±128.84	1,118.70	85 (39.91%)	125.91 ±180.52
4 – 5	189	43.19 ±109.74	866.15	67 (35.45%)	117.47 ±160.15
5 – 6	163	63.50 ±171.82	1,186.50	64 (39.26%)	157.64 ±247.19
6 – 7	94	116.41 ±561.36	5,229.08	38 (40.43%)	284.01 ±862.35
Total	1,338	46.10 ±201.08	5,229.08	446 (33.33%)	131.51 ±332.44

Supplementary Table 2. Free NE activity in the AREST CF early childhood cohort. Free NE activity was routinely measured in BALf collected from young children with CF at their annual assessment, using an adapted enzymatic assay. Both mean concentration and prevalence of detectable free NE activity increased with age. *Minimum detection limit for NE was 6.78 nM.

SUPPLEMENTARY FIGURES

Figure S1: Effect of free NE on cellular morphology of pAECs. Monolayer cultures of pAECs were exposed to 100 nM NE for 48 hours and time-lapse phase contrast images were collected. Both pAEC_{non-CF} (left column) and pAEC_{CF} (right column) monolayers demonstrated reduced cellular adhesion, cellular rounding and loss of confluence that progressed over 48 hours. Images representative of four separate experiments, shown at 10x magnification with inset images at 20x.

Figure S2: Effect of free NE on NuLi-1 and CuFi-1 cell confluence and viability. Monolayer cultures of hTERT transformed AEC were exposed to NE for 48 hours and then cell confluence, viability and cytotoxicity assessed. No change in confluence by NuLi-1 (A) and CuFi-1 (B) was observed in response to control media (circles), 10 nM (squares), 50 nM (triangles) and 100 nM (diamonds) NE. After 48 hours, assessment of viability by MTS assay (C) demonstrated that NuLi-1 (open bars) and CuFi-1 (closed bars) cell number was not reduced by NE. Nor was a significant change observed in the supernatant cytotoxicity marker LDH (D). Data was obtained from two to four separate experiments, with each point assessed in quadruplicate.

Figure S3: Effect of free NE on the morphology of proliferating pAEC_{non-CF}. Monolayer pAEC_{non-CF} cultures initially seeded at 5,000 cells/well were incubated for 24 hours to facilitate attachment and then subsequently exposed to NE over 120 hours. Time-lapse phase contrast images were then collected over this period at 2 hourly intervals.

Incubation with 100 nM NE resulted in a rounded morphology that indicated loss of cellular attachment. Also observed were fewer cell numbers at 120 hours, suggesting inhibition of proliferation. Images representative of four separate experiments, shown at 10x magnification with inset images at 20x.

Figure S4: Effect of free NE on the morphology of proliferating pAEC_{CF}. Monolayer pAEC_{CF} cultures initially seeded at 5,000 cells/well were incubated for 24 hours to facilitate attachment, then subsequently exposed to NE over 120 hours. Time-lapse phase contrast images were then collected over this period at 2 hourly intervals. Incubation with 100 nM NE resulted in a rounded morphology that indicated loss of cellular attachment. Also observed were fewer cell numbers at 120 hours, suggesting inhibition of proliferation. Images representative of four separate experiments, shown at 10x magnification with inset images at 20x.

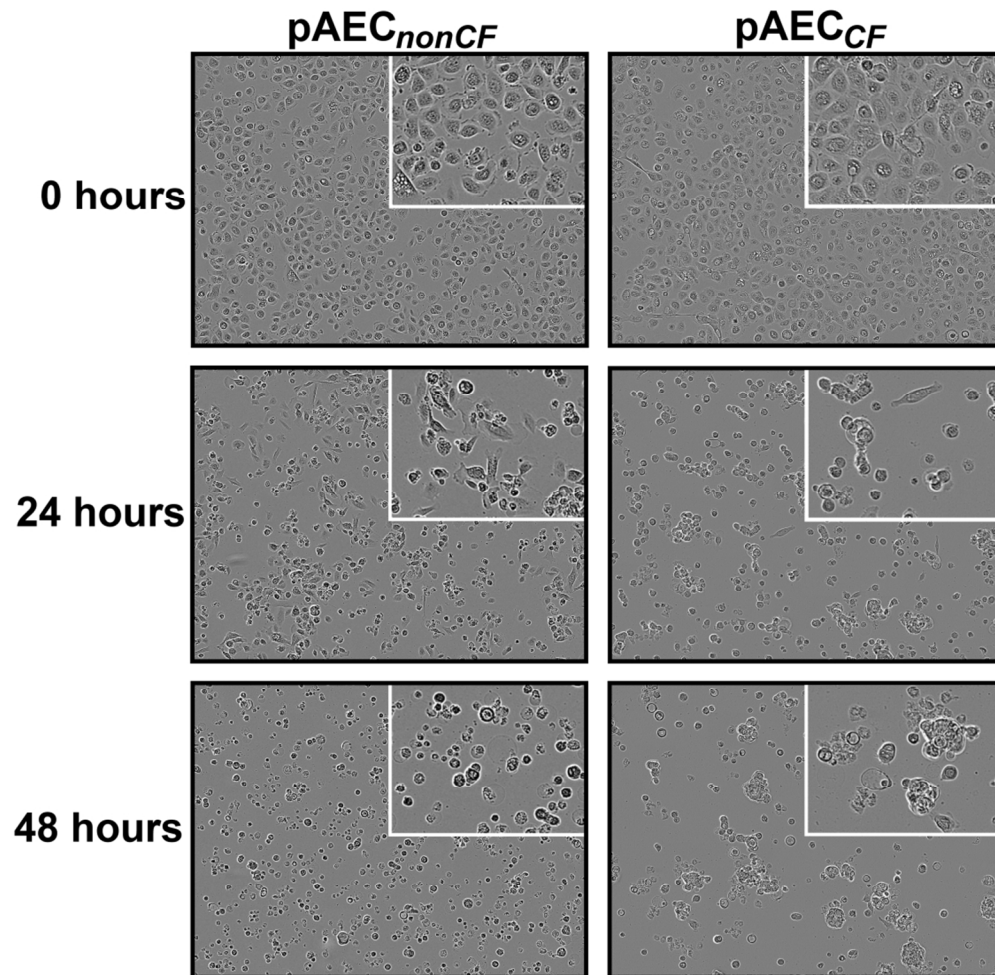
Figure S5: Effect of free NE on NuLi-1 and CuFi-1 cell proliferation. Monolayer hTERT transformed cell cultures initially seeded at 5,000 cells/well were incubated for four hours to facilitate attachment and then exposed to NE over 120 hours to assess effect on proliferation by measuring changes in confluence. When compared to control (circles), no change in confluence was seen by NuLi-1 (A) and CuFi-1 (B) in response to 10 nM (squares), 50 nM (triangles) and 100 nM (diamonds) NE. Assessment by MTS assay (C) demonstrated no effect on viable cell number of either NuLi-1 (open bars) or CuFi-1 (closed bars). Data was obtained from four separate experiments, with each point performed in triplicate.

Figure S6: Effect of α 1AT on pAEC_{CF} reattachment, resulting proliferation and wound repair. Confluent monolayer cultures of pAEC_{CF} were wounded with a single linear scratch (blue outline) and in the presence of 100 nM NE repair was assessed over 72 hours (left column), via the acquisition of time-lapse phase contrast images and analysis of pAEC_{CF} confluence (yellow highlight). At 12 hours post wounding, 1 μ M α 1AT was added certain wells to determine the effect on repair over the remaining 60 hours (right column). Data generated showed that, pAEC_{CF} treated with 1 μ M α 1AT progressively reattached to the culture vessel and induced significant wound coverage by 24 hours ($p < 0.05$). Repair continued to be significantly induced over 72 hours although not to completion ($p = 0.0008$). Images taken at 30 hours are representative of four separate experiments, shown at 10x magnification.

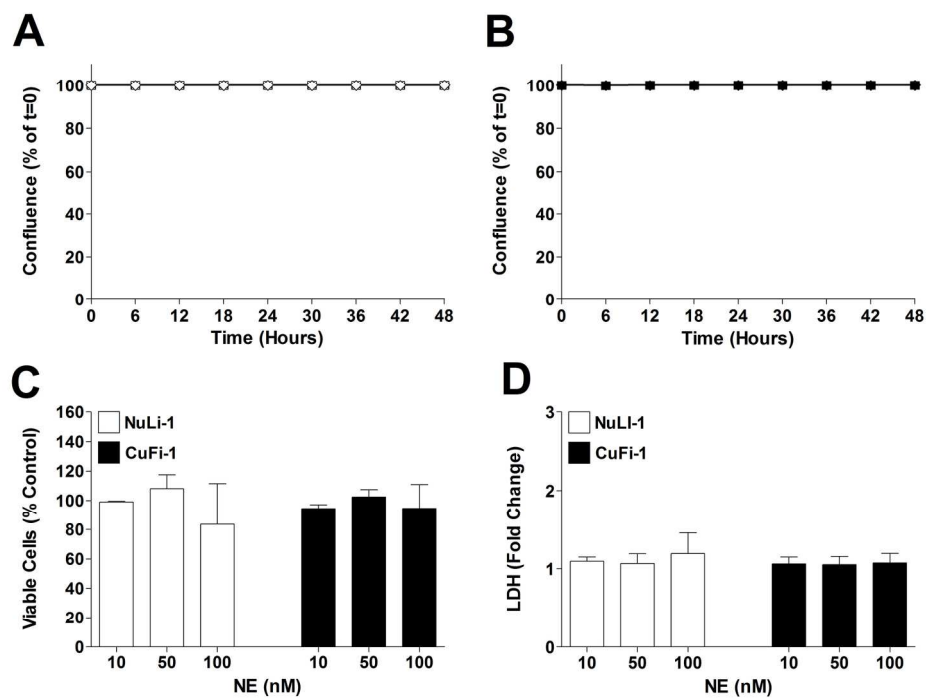
Figure S7: Effect of free NE on CuFi-1 wound repair. Confluent monolayer cultures of CuFi-1 were wounded with a single linear scratch and wound repair in the presence of control media (circles), 10 nM (squares), 50 nM (triangles) and 100 nM (diamonds) NE assessed. Wounded CuFi-1 in control media achieved 100% closure by 40 hours. However, 100 nM NE significantly reduced wound closure up to 42 hours post wounding. *indicates 100 nM NE $p < 0.05$ to control media. Data was collated from two separate experiments, with each point performed in quadruplicate.

References:

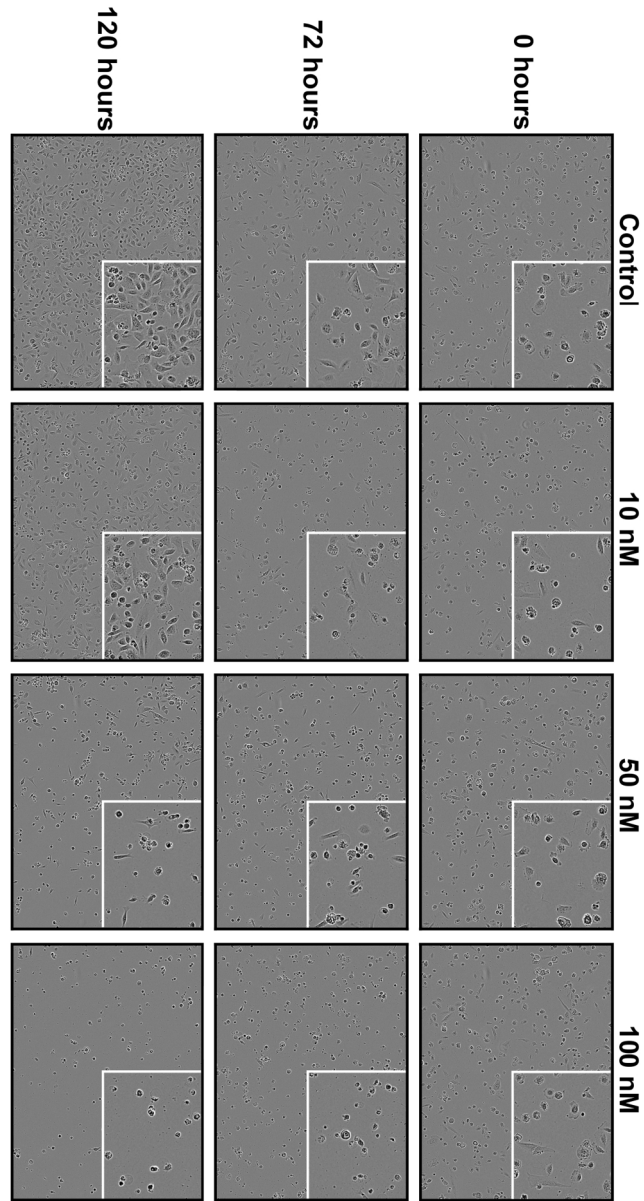
- E1. Berry LJ, Sheil B, Garratt L, Sly PD. Stability of interleukin 8 and neutrophil elastase in bronchoalveolar lavage fluid following long-term storage. *J Cyst Fibros* 2010;9(5):346-350.
- E2. Kicic A, Sutanto EN, Stevens PT, Knight DA, Stick SM. Intrinsic biochemical and functional differences in bronchial epithelial cells of children with asthma. *Am J Respir Crit Care Med* 2006;174(10):1110-1118.
- E3. Sutanto EN, Kicic A, Foo CJ, Stevens PT, Mullane D, Knight DA, Stick SM. Innate inflammatory responses of pediatric cystic fibrosis airway epithelial cells: Effects of nonviral and viral stimulation. *Am J Respir Cell Mol Biol* 2011;44(6):761-767.
- E4. Zabner J, Karp P, Seiler M, Phillips SL, Mitchell CJ, Saavedra M, Welsh M, Klingelutz AJ. Development of cystic fibrosis and noncystic fibrosis airway cell lines. *Am J Physiol Lung Cell Mol Physiol* 2003;284(5):L844-L854.
- E5. Cory AH, Owen TC, Barltrop JA, Cory JG. Use of an aqueous soluble tetrazolium/formazan assay for cell growth assays in culture. *Cancer Commun* 1991;3(7):207-212.
- E6. Huang KT, Chen YH, Walker AM. Inaccuracies in mts assays: Major distorting effects of medium, serum albumin, and fatty acids. *Biotechniques* 2004;37(3):406, 408, 410-412.
- E7. Ito Y, Shibata M-A, Kusakabe K, Otsuki Y. Method of specific detection of apoptosis using formamide-induced DNA denaturation assay. *J Histochem Cytochem* 2006;54(6):683-692.
- E8. Peterson MW, Walter ME, Nygaard SD. Effect of neutrophil mediators on epithelial permeability. *Am J Respir Cell Mol Biol* 1995;13(6):719-727.
- E9. Sundaram GM, Common JEA, Gopal FE, Srikanta S, Lakshman K, Lunny DP, Lim TC, Tanavde V, Lane EB, Sampath P. 'See-saw' expression of microrna-198 and fstl1 from a single transcript in wound healing. *Nature* 2013;495(7439):103-106.
- E10. Stick SM, Brennan S, Murray C, Douglas T, von Ungern-Sternberg BS, Garratt LW, Gangell CL, De Klerk N, Linnane B, Ranganathan S, et al. Bronchiectasis in infants and preschool children diagnosed with cystic fibrosis after newborn screening. *J Pediatr* 2009;155(5):623-628.e621.
- E11. Barrett AJ. Leukocyte elastase. *Methods Enzymol* 1981;80 Pt C:581-588.



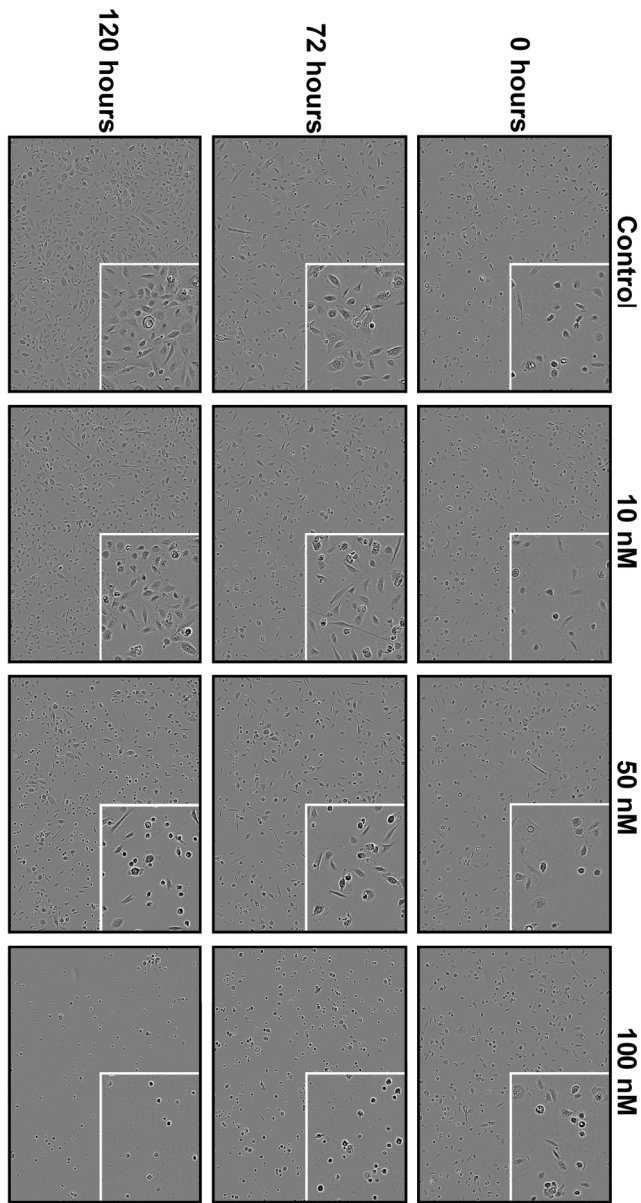
299x293mm (96 x 96 DPI)



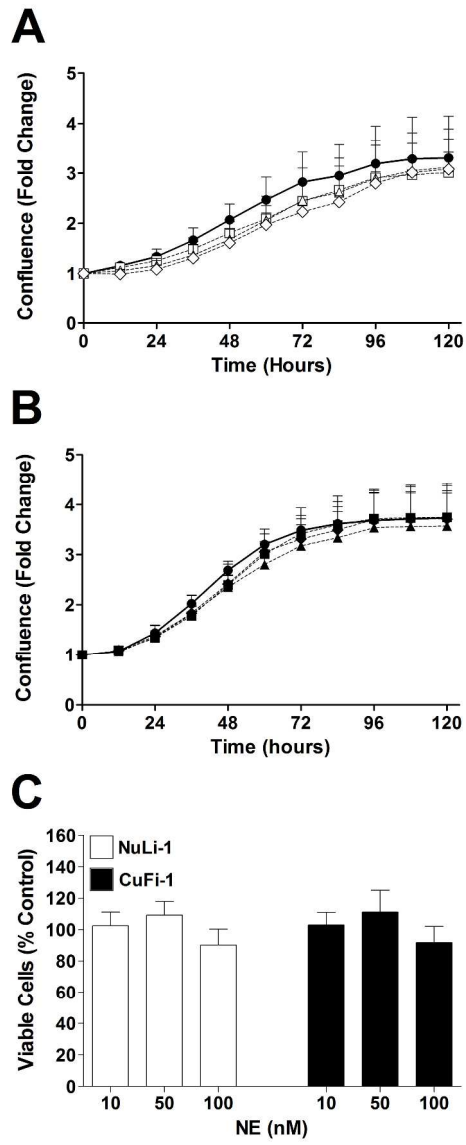
170x127mm (300 x 300 DPI)



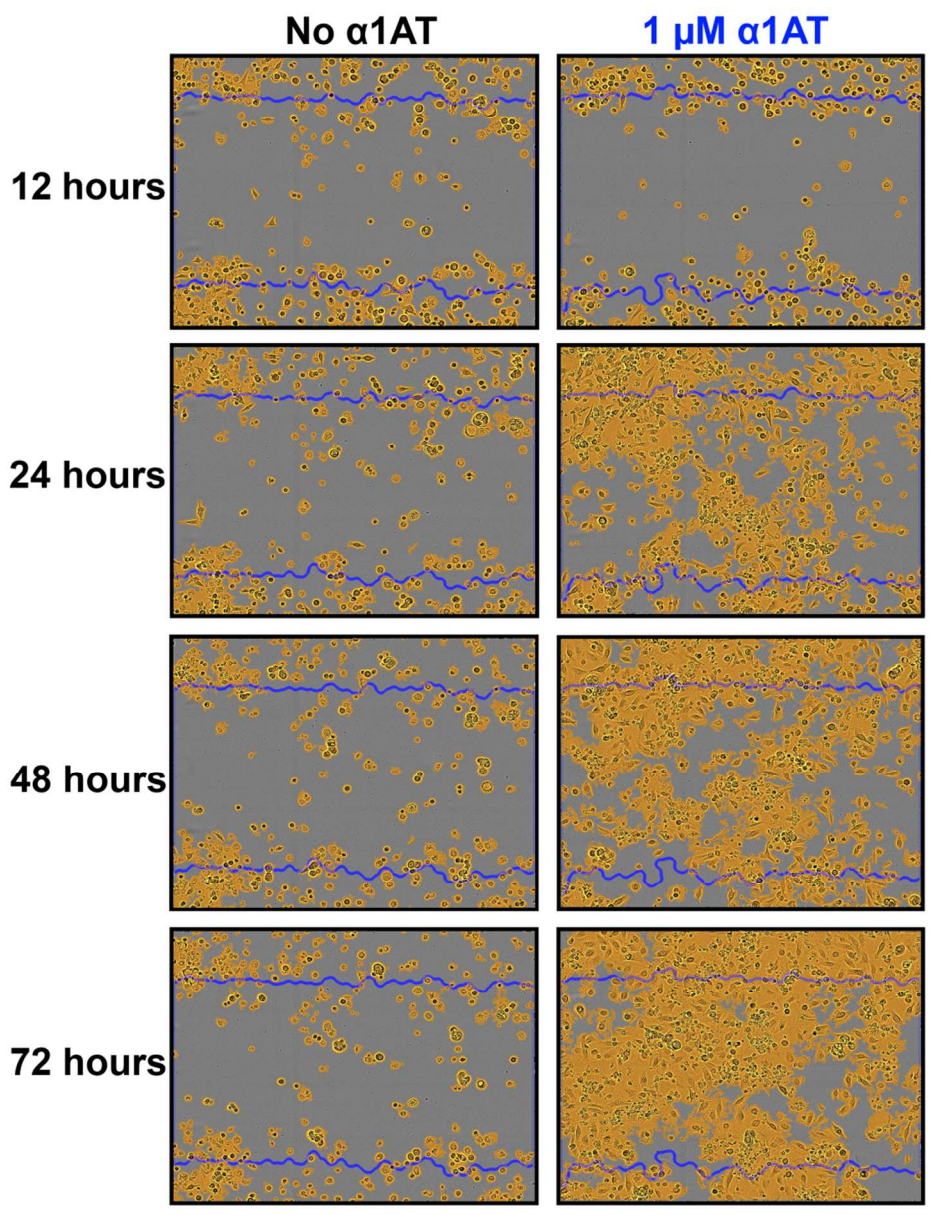
299x569mm (96 x 96 DPI)



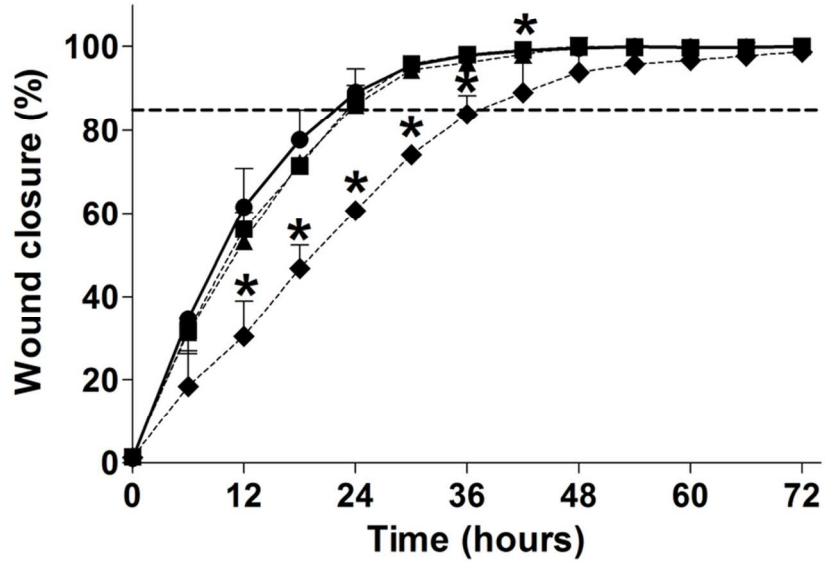
299x569mm (96 x 96 DPI)



261x567mm (300 x 300 DPI)



293x379mm (96 x 96 DPI)



83x57mm (300 x 300 DPI)